DOI: 10.58895/ksp/1000128686-7 erschienen in:
OCM 2021 - 5th International Conference on Optical Characterization of Materials, March 17th – 18th, 2021, Karlsruhe, Germany : Conference Proceedings
DOI: 10.58895/ksp/1000128686 | https://www.ksp.kit.edu/site/books/m/10.58895/ksp/1000128686/

Developing a handheld NIR sensor for the detection of ripening in grapevine

Lucie Gebauer[1], Julius Krause[2], Xiaorong Zheng[1], Felix Kronenwett[2], Robin Gruna[2], Reinhard Töpfer[1], and Anna Kicherer[1]

[1] Julius Kühn-Institut, Federal Research Centre of Cultivated Plants, Institute for Grapevine Breeding, Geilweilerhof, 76833 Siebeldingen
[2] Fraunhofer IOSB Institute of Optronics, System Technologies and Image Exploitation, Visual Inspection Systems, Fraunhoferstr. 1, 76131 Karlsruhe

Abstract It has already been proven that near infrared (NIR) reflectance spectroscopy can be used to measure the maturity of grapes by the determination of the sugar and acid content. Until now, winegrowers frequently collect a random one hundred berries sample per plot, to measure these parameters destructively for the estimation of the ideal harvest time of the gained product. Meanwhile, inexpensive sensors are available, to build convenient instruments for the non-destructive, low-priced and fast control of ripening parameters in the vineyard. For this, a small handheld device including a NIR sensor (1350 nm – 2600 nm) was built from a Raspberry Pi 3 single-board computer and a NIR sensor. Spectra of individual berries, sampled from Riesling (*Vitis vinifera*, L.) were collected. Corresponding reference data were determined with high performance liquid chromatography (HPLC). Samples were taken from different fruit as well as cluster zones and from the beginning of véraison until after harvest, to ensure a broad range of ingredients and the ripening properties of different berries from the vine. This study is the first that systematically investigates the ripening parameters of a whole vineyard with a handheld sensor. The sensor can be used in viticulture practice to detect the ripening progress and determining the ideal harvest time effective, simple, and non-destructively.

Keywords *Vitis vinifera*, Near Infrared Spectroscopy (NIRS), reflectance, ripening parameters, soluble solids, sugar, acid, handheld sensor, individual berry measurement

1 Introduction

Viticulture is of great economic importance worldwide with an estimated average productin of 258 million of hectoliters (Mio hl) of wine in 2020. In relation to global production, 60% were produced in Europe (156 Mio hl), while the USA (24.3 Mio hl), China (8.3 Mio hl) and Russia (4.6 Mio hl) are the leading countries outside of the European Union. Within Europe, Italy (47.5 Mio hl) is the largest wine producers followed by France (42.1 Mio hl), Spain (33.5 Mio hl), and Germany (9.0 Mio hl). Riesling is one of the widely grown white grapevine varieties worldwide, and in Germany the most important cultivar of about 23% (2019) of the wine grapes area. [1, 2]

One important factor to hold a large market share is the quality of the produced wine. While the proportion of table wine in Germany is relatively stable, the production of quality wine increases rapidly [1]. In order to obtain high quality grapes, the harvest time is of great importance, since after reaching the peak of ripening, over-ripening results in a decrease in quality. The growth of grape berry takes place in three phases consisting of two growth cycles and one lag-phase [3, 4]. After the lag-phase, from vérasion onwards, acids (mainly malic acid) slowly start to decrease while sugars increases rapidly. The presence and amount of mainly sugars and acids determines the quality and later characteristics of the wine, whereby the sugars are mainly represented by glucose and fructose and 70 % to 90 %, respectively, and the acid being mainly tartaric acid and malic acid [5–8]. Sugars determine the alcohol content of the later wine and acidity contributes to its fruity character. The balance of sugar and acidity are determining factors of typicity and wine style which is increasingly affected by climate change. [9] Due to uneven ripening on the cluster and on the grapevine, a winegrower in general collects one hundred berries, to estimate the average maturation of his vineyard. This process is destructive, laborious and to some extent error prone.

NIR sensors are already widespread in a wide variety of disciplines. They are used in medicine (blood oxygen, diabetes, intracranial bleeding), pharmacy or agriculture (particle measurements), and to ensure food quality. Till now, several vibrational spectroscopic methods were discovered to analyse different materials, based on the interaction of radiation with matter. The most prominent method is the FTIR, which is

based on the lowering of the radiation intensity due to infrared-active (IR-active) bonds. In contrast to the passing of light through the material, near infrared spectroscopy relies on the principle of reflection and absorption of radiation from the visible and near infrared spectrum of light (400 nm – 2500 nm). The IR-active bonds lower the reflection, resulting in an increase of the extinction coefficient (the degree of radiation attenuation), depicted as a peak in the reflection spectrum.

In order to investigate a feasible technique to detect quality attributes in crops, several sensors using IR radiation have been build for several fruits and vegetables. [10–12] Whilst some sensors measure the transmission spectrum of destroyed berries/bunches [13], other measure the diffuse reflection but with complex and expensive built ups with lamps and sensors. [14,15] Goisser *et al.* 2019 [16] developed a handheld NIR-sensor which measures diffuse reflection, by simply placing the fruit on the sensor. This technique could be used to classify the firmness and to determine sugar content of tomatoes.

Here, we built and investigated a handheld sensor to determine the most important quality attributes of an entire vineyard without having to repeatedly destroy grapes. With a few further developments, such as an app that can process the spectra immediately, we can give winemakers a simple and quick-to-use tool.

2 Material and methods

2.1 SmartSpectrometer system

The embedded spectrometer system *SmartSpectrometer* from Fraunhofer IOSB includes the spectrometer control and a real-time spectral processing unit with artificial intelligence. Furthermore, *SmartSpectrometer* provides a machine-to-machine interface based on OPC-UA (Open Platform Communications Unified Architecture) using the open source implementation open62541. This allows the system to be controlled remotely and additional sensors can be added. The built system consists of a FT-NIR sensor (NeoSpectra-Micro SWS 62231, Neospectra, SI-Ware, La Canada, California) mounted on a Raspberry Pi 3 (Raspberry Pi Foundation, Cambridge, United Kingdom) single-board computer. The sensors measures near infrared radiation in the range of 1350 nm - 2600 nm with a resolution of 16 nm.

The spectra of the berries were measured and recorded in the laboratory. A white and a black calibration was done with a Spectralon® reflection standard (Sphereoptics, Labsphere, Inc., North Sutton, NH), to minimize influence of the ambient light and background noise. Individual berries were dried with a paper towel, placed on the sensor, and five spectra from different sides of each berry were taken using a graphical user interface.

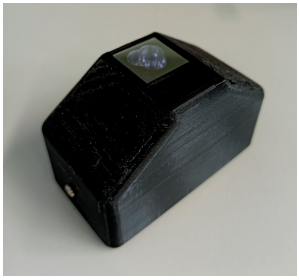

Figure 2.1: Handheld *SmartSpectrometer* device based on the NeoSpectra Micro development Kit. To determine the degree of maturity, the reflection spectrum is recorded non-destructively and evaluated directly in the embedded device.

2.2 Dataset

Grapevines of the variety Riesling (*Vitis vinifera*, L.) from four different locations in the individual vineyard site "Mütterle" in Wollmesheim (WH, Landau, Rhineland Palatinate, Germany) were used (see Fig. 2.2, Table 7.1). All vines were healthy, leaves and berries were free of damages. In the plots, vine and row spacing were comparable, the greening in the tracks was well-tended and rows were oriented north - south. All vines were trained in semi-arched canes and there were either one or two fruit zones, depending on height of the canopy, with a height of 30 cm to 50 cm per zone. Per vine and fruit zone two or four berries respectively were collected.

In total 512 individual berries were harvested. The sampling took place each week, beginning with véraison (08-17-2020) until harvest (09-28-2020) from defined vines, and one week after harvest (10-05-2020) from two to four vines in the field. Berries were taken from

defined but random selected vines, according their exposure to the sun (sun exposed, shaded), position in the cluster (near or far from the peduncle) and position at the vine (Table 7.1). Additionally, from each plot one hundred berries were randomly picked once a week from 08-10-2020 till harvest 09-28-2020, in order to determine the average maturity of the vineyard. Berries were transported to laboratory with a cooling box equipped with ice packs.

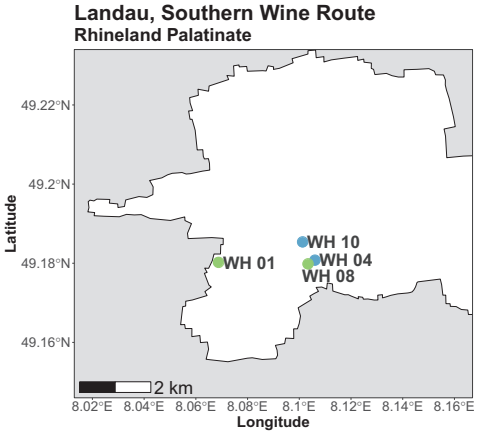

Figure 2.2: Wine growing areas in Wollmesheim (WH) near Landau, Rhineland Palatinate, Germany. Cultivar: *Vitis vinifera* (L.); variety: Riesling, individual vineyard site: Mütterle; farming practice: organic (green), conventional (blue).

Table 7.1: Rating data from the used Riesling areas in 2020 (Figure 2.2), created by the cooperative Deutsches Weintor; farming practice: organic (Org), conventional (Con); n.d.: not documented.

Abbreviation	Farming practice	Area (ha)	Planting year	Rootstock	Canopy height	Defoliation
WH 01	Org	13.32	2005	5C	1.10 m - 1.30 m	n.d.
WH 08	Org	48.60	1991	Binova	1.10 m - 1.30 m	none
WH 04	Con	48.67	1991	5C	> 1.30 m	one-sided
WH 10	Con	40.48	2006	5C	> 1.30 m	one-sided

2.3 Reference data

The juice for the measurement of the one hundred berries sample was obtained by mixing them with a commercial available mixer (BL 6280, Grundig, Germany). Individual berries were destroyed in a Falcon tube by shaking them with four metal bullets in a paint shaker (SK450 Fast and Fluid Management, Sassenheim, Netherlands). All Falcons were centrifuged at 25,419 · g in a cooled centrifuge (Sigma 6–16ks, Sigma, Kawasaki, Japan) to discard the cell debris. The juice was transferred, centrifuged with 12,100 · g (Minispin Eppendorf, Hamburg, Germany) again and 1:3 diluted with double distilled and filtered (pore size 0.2 nm) water. Amount of sugars and acids (glucose, fructose, malic- and tartaric acid) was determined using high performance liquid chromatography (Agilent 12900 Infinity 2, Agilent Technologies, Inc., Santa Clara, California) with ion-exchange ligand-exchange HiPlex H column (Agilent Technologies, Inc., Santa Clara, California), a refractive index detector for detection of carbohydrates and a diode array detector for acids. A standard series ranged from 1.5 to 90 g/L and 0.25 to 15 g/L for sugars and acids, respectively, was used. Recorded data were processed with Agilent OpenLab CDS Chemstation Software (Agilent Technologies, Inc., Santa Clara, California).

2.4 Least Squares Support Vector Regression

Due to the Beer-Lambert law, there is a non-linear relationship between the optical signal and a concentration of compounds, therefore Least Squares Support Vector Regression (LSSVR) with an RBF kernel was chosen as a non-linear regression method. The so-called kernel trick enables the estimation of non-linear correlations using LSSVR.

For the basic LSSVR the linear relation $y = \mathbf{w}\mathbf{x} + b$ between the regressors x and the dependent variable y is calculated by solving the following optimization problem

$$Q_{\mathrm{LSSVM}} = J(\mathbf{w}, \mathbf{e}) = \frac{1}{2}\mathbf{w}^T\mathbf{w} + \gamma \sum_{i=1}^{n} e_i^2 \tag{2.1}$$

subject to the equality constraints

$$y_i - \mathbf{w}^T\mathbf{x}_i - b = e_i, \qquad i = 1, 2, ..., l \tag{2.2}$$

where γ is the regularization parameter and e_i is the regression error. The advantage of the LSSVR over the regular SVM is provided via converting a quadratic programming problem into a set of linear equations. By constructing the Lagrange function with the Lagrange multipliers α, a set of conditions for optimality can be derived. This leads to a set of linear equations that needs to be solved to obtain the parameters α and b. The resulting LSSVM model used in function estimation is

$$y_i = \sum_{i=1}^{n} \alpha_i K(\mathbf{x}, \mathbf{x}_i) + b \tag{2.3}$$

with the RBF kernel function K. For the model calculation the regularization parameter γ and the bandwidth of the RBF kernel σ needs to be chosen [17].

3 Results and discussion

Reference data were evaluated and depicted using R (Version 3.6.1) [18] and R-Studio [19], as well as the packages ggplot2 [20] and Rmisc [21]. Spectral data analysis and modelling was performed using the spectraltoolbox framework from Fraunhofer IOSB based on Python 3.8.

3.1 Reference data for spectral data processing

The sugar (glucose, fructose) and acid (tartaric -, malic acid) contents of berries were measured with high performance liquid chromatography (HPLC) and results of hundred berries samples are depicted in Figure 3.1.

In individual berries, sugar contents ranged from 6.59 g/l to 115.58 g/l and from 11.52 g/l to 108.83 g/l for glucose and fructose, respectively, over the entire ripening process. For acids, ranges were smaller and high values were gained at the begin of the ripening with 15.45 g/l for tartaric and 21.79 g/l for malic acid, respectively. While the malic acid was partially almost completely metabolized, minimum tartaric acid content was 3.93 g/l.

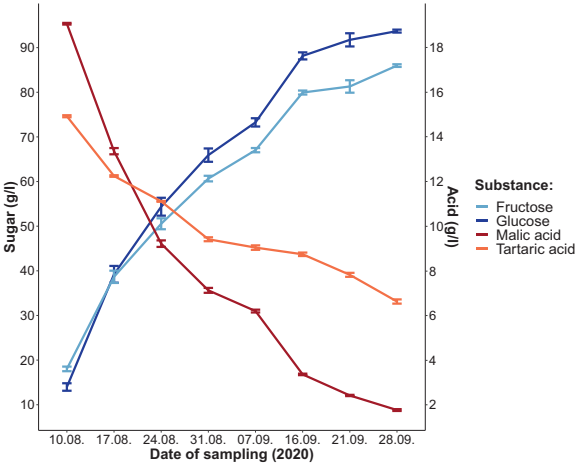

Figure 3.1: Sugar and acid contents in the hundred berries samples, measured with HPLC, error bars correspond to standard errors, each data point represents the mean of the four parcels.

3.2 NIR data analysis

The data set contains spectral data from four plots at different locations. The validation is performed like the later use-case of the ripeness estimation of a plot at a specified date. Therefore, the plot used for validation was not included in the training and the median of all predictions is used.

The evaluation of the spectral data was done in several steps. First, spectra with a low signal strength (average intensity below 0.04) were discarded. Subsequently, the intensities of the spectral data were normalised using Standard Normal Variate (SNV) [22]:

$$x_{\text{snv}} = \frac{x - \bar{x}}{\sigma_x} \tag{3.1}$$

As a metric to evaluate the regression model, the RMSE and R^2 score is used. The RMSE score

$$\text{RMSE} = \sqrt{\frac{\sum_{i=1}^{n} (\hat{y}_i - y_i)^2}{n}} \tag{3.2}$$

estimates the standard deviation of the prediction of a regression model. A distinction can be made between the RMSE of prediction and the RMSE of calibration, depending on y_i used during calculation. In addition, the R2 score

$$R^2 = 1 - \frac{\sum_{i=1}^{n}(e_i^2)}{\sum_{i=1}^{n}(y_i - \bar{y})^2} \tag{3.3}$$

indicates how well the independent variables are suited to explain the variance of the dependent variables. In both formulas n is the number of observations.

Due to the lack of sample preparation, the measurement in reflection with low signal strength and the use of miniaturised low-cost sensors, there is an enhanced measurement uncertainty. Because the prediction of the entire plot at a point in time are relevant for the winemaker, stochastic errors and outliers can be reduced very well by determining the median of the single berry predictions. The quality of the prediction of individual grape berries in the training and the median of the prediction of the validation plot at each time point is shown in Table 7.2.

It can be clearly seen that the median of the single berry prediction leads to very good results. More precisely, Figure 3.2 shows the median of acid and sugar of the measured individual berries at different time points. With this model we were able to determine glucose and fructose content with 87 % accuracy ($\pm$7.59 g/l and $\pm$6.57 g/l, respectively) and tartaric, as well as malic acid with 89 % and 78 % accuracy ($\pm$0.52 g/l and $\pm$1.89 g/l, respectively). Compared to previous studies that measured the total soluble solids, we were able to predict two individual sugars with a high degree of accuracy [23, 24]. The two selected acids could also be predicted separatly, with a better forcast for tartaric acid, which is the prevalent acid at harvest [23, 25]. Higher precision could eventually be achieved with other models, for which more data are to be collected.

Table 7.2: Results of the spectral evaluations using LSSVR. Shown are root mean square errors of calibration ($RMSE_C$) from the training set, the root mean square error of the median prediction ($RMSE_P$) from validation set, the degree of determination (R^2).

Validation		training individual grape berries		validation median prediction	
Plot	Compound	$RMSE_C$	R^2	$RMSE_P$	R^2
WH 01	Glucose	5.29	0.94	9.90	0.87
	Fructose	4.48	0.94	8.75	0.86
	Tartaric acid	0.51	0.93	1.80	0.54
	Malic acid	1.02	0.93	2.11	0.84
WH 04	Glucose	5.21	0.94	7.59	0.87
	Fructose	4.48	0.94	6.57	0.87
	Tartaric acid	0.68	0.90	0.52	0.89
	Malic acid	1.06	0.93	1.89	0.78
WH 08	Glucose	5.34	0.94	8.70	0.78
	Fructose	4.63	0.94	7.98	0.77
	Tartaric acid	0.61	0.91	1.17	0.62
	Malic acid	0.98	0.94	1.40	0.86
WH 10	Glucose	5.67	0.93	10.14	0.80
	Fructose	4.83	0.93	8.47	0.81
	Tartaric acid	0.63	0.91	1.25	0.59
	Malic acid	1.09	0.93	1.37	0.86

4 Summary

Sugar (alcohol) and acid content of grapes have a huge impact on the sensory perception of wine. Measuring of these ingredients is a proxy for ripening of a vineyard.

Proof of concept was provided on applying a miniature sensor to measure the maturity of Riesling in vineyards with high accuracy. In view of the application in the vineyard, the prototype offers an option for monitoring the ripening in a time efficient way. It is expected that the sensor will be manageable with one hand. If an App for mobile phones is developed, the results of the measurement will become immediately apparent. The alternative to invasive measurements being laborious e.g. a handheld sensor to quantify sugars and acids non-invasively on hundreds of berries is a step forward towards digitalization and precision viticulture.

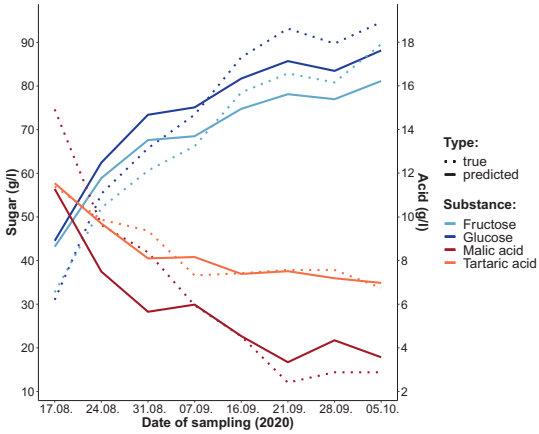

Figure 3.2: Median of determined (true, solid line) and estimated (predicted, dashed line) sugar and acid contents in single berries of the plot WH 04.

Acknowledgement

The study is supported by funds of the Federal Ministry of Food and Agriculture (BMEL) based on a decision of the Parliament of the Federal Republic of Germany via the Federal Office for Agriculture and Food (BLE), within the frame work DigiVine (FKZ: 28DE113A18). We also thank Ann-Kathrin Ickert and Maximilian Mathes for technical support and Michael Straube from the cooperative Deutsches Weintor e.G. for arranging experimental areas from winegrowers and corresponding rating data.

References

1. Deutsches Weininstitut GmbH, "Deutscher Wein Statistik 2020/2021," 2020. [Online]. Available: www.deutscheweine.de,www.germanwines.de
2. OIV, "Weinerzeugung 2020, statusbericht der oiv - erste schätzungen." [Online]. Available: http://www.oiv.int/public/medias/7548/de-weinerzeugung-2020-oiv-erste-sch-tzungen.pdf
3. B. G. Coombe, "Relationship of growth and development to changes in

sugars, auxins, and gibberilins in fruit of seeded and seedless varieties of vitis vinifera," *Plant Physiology*, vol. 35, no. 2, pp. 241–250, 1960.

4. B. G. Coombe and C. R. Hale, "The hormone content of ripening grape berries and the effects of growth substance treatments," *Plant Physiology*, no. 51, pp. 629–634, 1973.
5. C. Conde, P. Silva, N. Fontes, A. C. P. Dias, R. M. Tavares, M. J. Sosua, A. Agasse, S. Delrot, and H. Gerós, "Biochemical changes throughout grape berry development and fruit and wine quality," *Global Science Books*, vol. 1, no. 1, pp. 1–22, 2007.
6. H.-F. Liu, B.-H. Wu, P.-G. Fan, S.-H. Li, and L.-S. Li, "Sugar and acid concentrations in 98 grape cultivars analyzed by principal component analysis," *Journal of the Science of Food and Agriculture*, vol. 86, no. 10, pp. 1526–1536, 2006.
7. R. B. Beelman and J. F. Gallander, "Wine deacidification," ser. Advances in Food Research. Elsevier, 1979, vol. 25, pp. 1–53.
8. H. P. Ruffner, "Metabolism of tartaric and malic acids in vitis_ a review - part a," *Vitis*, vol. 21, pp. 247–259, 1982.
9. R. Mira de Orduña, "Climate change associated effects on grape and wine quality and production," *Food Research International*, vol. 43, no. 7, pp. 1844–1855, 2010.
10. D. Cozzolino, R. Dambergs, L. Janik, and W.U. Cynkar and M. Gishen, "Review: Analysis of grapes and wine by near infrared spectroscopy," *Journal of Near Infrared Spectroscopy*, no. 14, pp. 279–289, 2006.
11. D. Cozzolino, W. Cynkar, N. Shah, and P. Smith, "Technical solutions for analysis of grape juice, must, and wine: the role of infrared spectroscopy and chemometrics," *Analytical and bioanalytical chemistry*, vol. 401, no. 5, pp. 1475–1484, 2011.
12. C. A. T. dos Santos, M. Lopo, R. N. M. J. Páscoa, and J. A. Lopes, "A review on the applications of portable near-infrared spectrometers in the agro-food industry," *Applied spectroscopy*, vol. 67, no. 11, pp. 1215–1233, 2013.
13. J. Fernández-Novales, M.-I. López, M.-T. Sánchez, J. Morales, and V. González-Caballero, "Shortwave-near infrared spectroscopy for determination of reducing sugar content during grape ripening, winemaking, and aging of white and red wines," *Food Research International*, vol. 42, no. 2, pp. 285–291, 2009.
14. A. J. Daniels, C. Poblete-Echeverría, U. L. Opara, and H. H. Nieuwoudt, "Measuring internal maturity parameters contactless on intact table grape

bunches using nir spectroscopy," *Frontiers in plant science*, vol. 10, p. 1517, 2019.

15. H. Abdul Rahim, K. S. Chia, and R. Abdul Rahim, "Visible and near infrared (vir-nir) spectroscopy: Measurement ans prediction of soluble solid content of apple," *Sensors & Transducers Journal*, vol. 121, no. 10, pp. 42–498, 2010.
16. S. Goisser, J. Krause, M. Fernandes, and H. Mempel, "Determination of tomato quality attributes using portable nir-sensors: Conference paper," 2019.
17. J. A. K. Suykens, L. Lukas, and J. Vandewalle, "Sparse approximation using least squares support vector machines," in *2000 IEEE International Symposium on Circuits and Systems (ISCAS)*, vol. 2, 2000, pp. 757–760.
18. R Core Team, *R: A Language and Environment for Statistical Computing*, R Foundation for Statistical Computing, Vienna, Austria, 2019. [Online]. Available: https://www.R-project.org
19. RStudio Team, *RStudio: Integrated Development Environment for R*, RStudio, Inc., Boston, MA, 2019. [Online]. Available: http://www.rstudio.com/
20. H. Wickham, *ggplot2: Elegant Graphics for Data Analysis*. Springer-Verlag New York, 2016. [Online]. Available: https://ggplot2.tidyverse.org
21. R. M. Hope, *Rmisc: Ryan Miscellaneous*, 2013, r package version 1.5. [Online]. Available: https://CRAN.R-project.org/package=Rmisc
22. A. Rinnan, F. van den Berg, and S. B. Engelsen, "Review of the most common pre-processing techniques for near-infrared spectra," *TrAC Trends in Analytical Chemistry*, vol. 28, no. 10, pp. 1201–1222, 2009.
23. F. Antonucci, F. Pallottino, G. Paglia, A. Palma, S. D'Aquino, and P. Menesatti, "Non-destructive estimation of mandarin maturity status through portable vis-nir spectrophotometer," *Food and Bioprocess Technology*, vol. 4, no. 5, pp. 809–813, 2011.
24. S. Lee, S. Sarkar, Y. Park, J. Yang, and G. Kweon, "Feasibility study for an optical sensing system for hardy kiwi (actinidia arguta) sugar content estimation," *Journal of Agriculture & Life Science*, vol. 53, no. 3, pp. 147–157, 2019.
25. R. Beghi, A. Mena, V. Giovenzana, R. Civelli, S. Best, L. F. Leòn Gutiérrez, and R. Guidetti, "Quick quality evaluation of chilean grape by a portable vis/nir device," *Acta Horticulturae*, no. 978, pp. 93–100, 2013.